Enhanced nitrogen loss from rivers through coupled nitrification-denitrification caused by suspended sediment

Xinghui Xia [a,*], Ting Liu [a], Zhifeng Yang [a,*], Greg Michalski [b,*], Shaoda Liu [c], Zhimei Jia [a], Sibo Zhang [a]

[a] School of Environment, Beijing Normal University/State Key Joint Laboratory of Environmental Simulation and Pollution Control, Beijing 100875, China
[b] Department of Earth, Atmospheric and Planetary Sciences, Purdue University, West Lafayette, IN 47907, United States
[c] Department of Geography, National University of Singapore, 1 Arts Link, Kent Ridge 117570, Singapore

HIGHLIGHTS

- Coupled nitrification-denitrification can occur around SPS in oxic waters.
- $^{15}N_2$ production rate from $^{15}NH_4^+$ increased with SPS concentration as a power function.
- Nitrifying and denitrifying bacteria population increased with SPS as a power function.
- $1\ g\ L^{-1}$ SPS will lead to N-loss enhancement by approximately 25–120%.
- N-loss enhancement caused by SPS increased with organic carbon content of SPS.

GRAPHICAL ABSTRACT
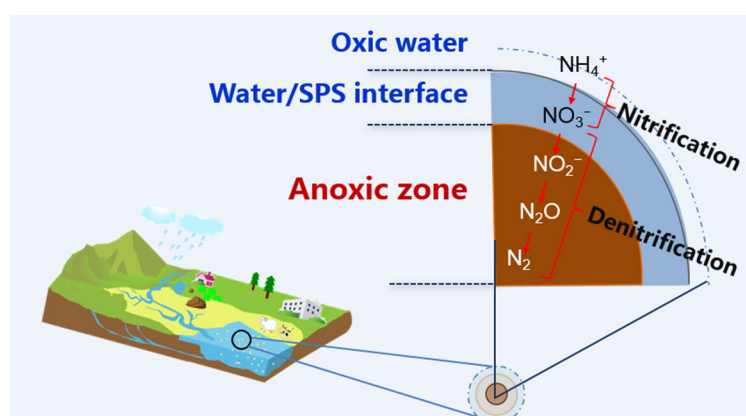
ABSTRACT

Present-day estimations of global nitrogen loss (N-loss) are underestimated. Commonly, N-loss from rivers is thought to be caused by denitrification only in bed-sediments. However, coupled nitrification-denitrification occurring in overlying water with suspended sediments (SPS) where oxic and anoxic/low oxygen zones may coexist is ignored for N-loss in rivers. Here the Yellow and Yangtze Rivers were taken as examples to investigate the effect of SPS, which exists in many rivers of the world, on N loss through coupled nitrification-denitrification with nitrogen stable (^{15}N) isotopic tracer simulation experiments and in-situ investigation. The results showed even when SPS was surrounded by oxic waters, there were redox conditions that transitioned from an oxic surface layer to anoxic layer near the particle center, enabling coupled nitrification-denitrification to occur around SPS. The production rate of $^{15}N_2$ from $^{15}NH_4^+$-N ($R_{15N2\text{-production}}$) increased with increasing SPS concentration ([SPS]) as a power function ($R_{15N2\text{-production}} = a \cdot [SPS]^b$) for both the SPS-water and bed sediment-SPS-water systems. The power-functional increase of nitrifying and denitrifying bacteria population with [SPS] accounted for the enhanced coupled nitrification-denitrification rate in overlying water. SPS also accelerated denitrification in bed-sediment due to increased NO_3^- concentration caused by SPS-mediated nitrification. For these two rivers, $1\ g\ L^{-1}$ SPS will lead to N-loss enhancement by approximately 25–120%, and the enhancement increased with

* Corresponding authors.
 E-mail addresses: xiaxh@bnu.edu.cn (X. Xia), zfyang@bnu.edu.cn (Z. Yang), gmichals@purdue.edu (G. Michalski).

organic carbon content of SPS. Thus, we conclude that SPS in overlying water is a hot spot for nitrogen loss in river systems and current estimates of in-stream N-loss are underestimated without consideration of SPS; this may partially compensate for the current imbalance of global nitrogen inputs and sinks.

1. Introduction

Nitrogen (N), a major element required by all organisms, is widely applied in industry, agriculture, and domestic activities, but excess N can cause eutrophication and hypoxia in water bodies, destruction of habitats for resident organisms, and reduction of species diversity (Lenihan and Peterson, 1998; Mallin et al., 2006; Liu et al., 2013a; Roberts et al., 2014). Therefore, understanding the processes controlling N budget, such as the N fixation, assimilation, nitrification, and denitrification is vital. Yet, despite decades of research, the global N budget remains out of balance, with inputs exceeding losses (Galloway, 1998; Gruber and Galloway, 2008; Schlesinger, 2009). This imbalance indicates that some unknown processes might contribute to N losses, thus resulting in major uncertainties in model simulations and limiting the accuracy of forecasts of future river N export caused by climate change, urbanization, and human population growth.

Rivers are subject to high loads of nitrogen and can convert approximately 40% of terrestrial nitrogen (N) runoff (~47 Tg per year) to biologically unavailable dinitrogen gas (Galloway et al., 2004). Nitrogen loss from rivers plays an important role for N delivery to coastal ecosystems (Donner and Kucharik, 2008), which often controls eutrophication and the development of pelagic "dead zones" (Turner and Rabalais, 1994; Rabalais, 2002; Diaz and Rosenberg, 2008). Studies of N loss from river systems have mainly focused on bed-sediment denitrification which is currently considered as the main in-stream N loss process (Boyer et al., 2006; Johannsen et al., 2008; Li et al., 2010; Liu et al., 2013b). Nitrification, the aerobic oxidation of NH_4^+ to NO_3^- via NO_2^- performed primarily by ammonia-oxidizing bacteria and archaea, is an important nitrate supply that is subsequently transported to anaerobic zones in bed-sediments and reduced by denitrification in river systems (Seitzinger, 1988; Pina-Ochoa and Álvarez-Cobelas, 2006; Mulholland et al., 2008; Liu et al., 2013b). This suggests that nitrification and denitrification in rivers might be tightly coupled, however the timescale of nitrate diffusion at the water-sediment interface is thought to limit the role of bed-sediment denitrification in river systems (Venterink et al., 2003; O'Connor and Hondzo, 2007).

Although several studies suggested that coupled nitrification-denitrification (CND) might occur in water column of some estuaries with high turbidity (Abril et al., 2000; Sebilo et al., 2006), N loss in river systems by CND occurring in water column containing suspended sediments (SPS) where possible anoxic/low oxygen microsites may exist has been largely ignored. SPS exists in many rivers around the world (Mulder and Syvitski, 1995; Sivakumar, 2002; Billi and Ali, 2010; Water Conservancy Committee of the Yellow River, 2013), and it has been shown that nitrification rates increase with SPS concentration (Xia et al., 2004, 2009, 2013). Additionally, it has been proven that denitrification rate increases linearly with SPS concentration in oxic waters according to the results of incubation experiment with added $^{15}NO_3^-$-N (Liu et al., 2013b), and Reisinger et al. (2016) found denitrification occurring in the water column of certain rivers. The anoxic/low oxygen microsites were assumed to exist in suspended particles surrounded by oxidized waters according to the theories of transport limitations and multispecies biofilms (Lamontag et al., 1973; Bianchi et al., 1992; Michotey and Bonin, 1997; Falkowski et al., 2008). Building on these recent findings, we hypothesized that a gradient of oxic and anoxic/low oxygen conditions exists within SPS particles with oxic conditions at the surface layer and anoxic/low oxygen conditions near the center of particle. Then CND could occur in oxic waters in the presence of SPS, with nitrification occurring at the surface layer and

denitrification occurring in the inner layer of SPS. In addition to providing oxygen-limited microsites for denitrification, SPS will also accelerate river denitrification rates by generating more NO_3^- from SPS, which increases NO_3^- concentration gradients between overlying water and bed-sediment and thus enhances diffusion rates, promoting bed-sediment denitrification in river systems.

Therefore, we hypothesized that there will be enhanced N-loss through CND and other nitrogen transformation processes in river systems where there are significant amounts of SPS. The influences of SPS concentration on N loss in the Yellow River and the Yangtze River were investigated using isotopic and chemical techniques; the SPS concentration of these two rivers ranged from 0.01 to 54.8 g L^{-1} and from 0.01 to 10.5 g L^{-1}, respectively (Changjiang Water Resource Committee, 2014; Xia et al., 2016). In detail, the present study aimed to: 1) examine whether CND could occur at SPS particles, and explore the relevant mechanisms; 2) investigate and model the relationship between CND rate and SPS concentration; 3) estimate the impacts of enhanced CND by SPS on N-loss from river systems.

2. Materials and methods

2.1. Sample collection

Sediment and water samples used in incubation experiments were collected from five sites including Longmen (LM, 110°36′06.4″E, 35°39′33.9″N), Huayuankou (HYK, 113°41′07.7″E, 34°54′16.8″N), and Aishan (AS, 116°16′39.7″E, 36°13′44.4″N) Stations in the Yellow River and 37-Dock (37-Dock, 114°20′09.5″E,30°36′30.5″N) and Wanzhou (WZ, 108°22′56.30″E, 30°48′39.85″N) Stations in the Yangtze River (Fig. 1). To avoid being contaminated by surface pollutants, water samples at 0.2 m below the water surface were collected with a TC-Y sampler (TECH Instrument in Shenyang, China), and analyzed for properties including the content of organic carbon and nitrogen species (see below). The top 10-cm bed-sediment samples, which are more easily resuspended during flow fluctuation, were collected with a sediment grab sampler. In addition, SPS and water samples were collected from 17 sites of the Yellow River to study the effect of SPS concentration on in-situ nitrifying and denitrifying bacteria abundances (Fig. 1). Then all the above samples were kept under 4 °C in a cooler and shipped to laboratory for further analysis. Incubation experiments began within 48 h after sampling. The sediment characteristics at the five sampling sites of the Yellow River and the Yangtze River are shown in Table 1.

2.2. Incubation of SPS-water systems with various SPS concentrations

Taking the samples collected from site AS as an example to examine whether CND could occur on SPS particles, a set of chambers containing SPS and water but no bed-sediment were designed. The experimental design was similar to our previous study (Liu et al., 2013b). A series of chambers containing 800-ml artificial overlying water with 5 mgL^{-1} $^{15}NH_4^+$-N as $^{15}NH_4^+$Cl (99.0 atm% ^{15}N, Shanghai Research Institute of Chemical Industry, China) were designed to obtain a 20-cm-deep water column. The artificial overlying water contained indigenous bacteria in the Yellow River and its preparation is shown in Supplementary Section S1. Triplicate experiments were conducted for each incubation set. A certain amount (0, 0.8, 2, 6.4, 12 and 16 g) of homogenized bed-sediment was respectively added into each chamber, which were then incubated at 25 °C. All the added sediment was suspended by setting agitation rates at 50, 150, 200, 400, 550, and 700 r min^{-1}, obtaining SPS
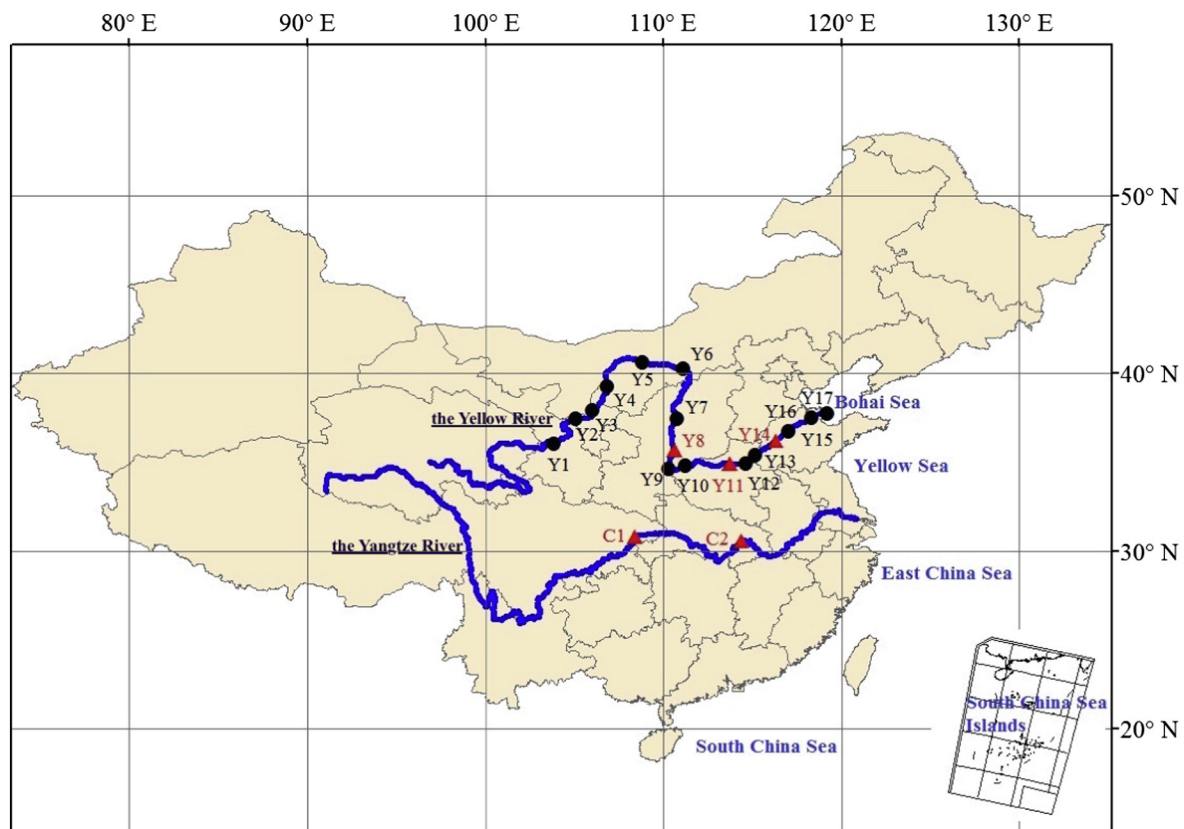
Fig. 1. The sampling sites of the Yellow River and the Yangtze River. Red triangles mark sampling sites for simulation experiments (Y8: Longmen = LM, Y11: Huayuankou = HYK, Y14: Aishan = AS; C1: Wanzhou = WZ, C2: 37-Dock), and black circles represent locations for investigation of *in-situ* bacteria abundances (Y1: Lanzhou, Y2: Xiaheyan, Y3: Qingtongxia, Y4: Shizuishan, Y5: Sanhuhekou, Y6: Toudaoguai, Y7: Wubao, Y9: Tongguan, Y10: Sanmenxia, Y12: Kaifeng, Y13: Gaocun, Y15: Luokou, Y16: Lijin, Y17: Kenli). (For interpretation of the references to color in this figure legend, the reader is referred to the web version of this article.)

concentrations of 0, 1, 2.5, 8, 15, and 20 g L^{-1}, respectively. The chemical conditions of water in each chamber were the same (Supplementary Table S1), and they are similar to that of river water. At pre-determined intervals (every three days), gas from headspace produced during each incubation period was sampled using a gas-tight syringe for the measurement of δ^{15}N-N_2, and then the concentration excess ^{15}N-N_2 was calculated. The remaining ^{15}N$_2$ produced during previous incubation period was purged by aerating the water phase for 30 min, and the aeration also helped keep oxygen level at saturation. The dissolved oxygen concentration was determined after each sampling and it was approximately 8.2 mg L^{-1} during experiment. At the end of experiment, sediment and water were separated by letting the sediment settle out, and the density of denitrifying bacteria in the SPS and water samples was measured using the most-probable-number-PCR (MPN-PCR) method (Section 2.6 and Supplementary Section S3). The control sets were performed using sterilized sediment and water samples, and mercuric chloride was added to the control sets with a final concentration of 0.5% to inhibit the microbial activities. The production of ^{15}N$_2$ caused by microbial activities was calculated by subtracting ^{15}N$_2$ produced in the control systems from that in each incubation set.

In addition, the mechanisms accounting for the occurrence of CND on SPS particles were analyzed by examining the O_2 flux and profile around the SPS particle. To do this, one more set of chambers containing 800 mL solution with 5 mg L^{-1} NH_4^+-N and 20 g L^{-1} SPS of different sizes (<20 μm, 20–50 μm, 50–100 μm, and >100 μm), which were separated by wet screening and sedimentation methods using samples collected from the site AS, were incubated at 25 °C. The detection of O_2 flux and profile around SPS particles was performed using Non-invasive Micro-test Technology and microelectrode technology (Jaffe and Nuccitelli, 1974; Revsbech, 1989; Smith, 1995), respectively. The details for the determination are described in Supplementary Section S2.

2.3. Incubation of bed sediment-SPS-water system with various SPS concentrations

A 10-cm-deep sediment column was constructed by adding a certain amount of homogenized bed-sediment into the gastight polymethyl methacrylate (PMMA) incubation chambers, as described by Liu et al. (2013b). Then the sediment was covered by 800 mL artificial overlying water with 5 mg L^{-1} ^{15}NH$_4^+$-N. Triplicate experiments were conducted

Table 1
Summary of sediment characteristics at the five sampling sites of the Yellow River and the Yangtze River.

Site name	River	Particle size (%)				TOC		Total organic nitrogen
		<20 μm	20–50 μm	50–100 μm	>100 μm	(%)		(%)
Huayuankou	The Yellow River	2.9	22.8	37.5	19.9	0.167		0.02
Longmen	The Yellow River	4.0	24.9	50.8	15.8	0.186		0.01
Aishan	The Yellow River	23.2	46.4	25.1	4.3	0.215		0.02
37-Dock	The Yangtze River	23.0	18.6	35.9	16.0	0.599		0.05
Wanzhou	The Yangtze River	55.7	17.4	12.7	6.1	0.668		0.06

for each incubation set. The SPS concentrations were set at 20, 15, 8, 2.5, 1, and 0 g L^{-1} by adjusting the agitation rates at 700, 550, 400, 200, 150, and 0 r min^{-1} respectively, simulating the real rivers containing different concentrations of SPS. The variation of measured SPS concentration in each chamber was <5% of the pre-set one. The particle size of SPS in the systems containing different concentrations of SPS was similar to that of SPS in real rivers (Supplementary Table S2). All the chambers were incubated at 25 °C. At pre-determined intervals (every one to three days), water samples were sucked out of the chamber using a columnar sampler as described in Liu et al. (2013b); the other procedures including gas sampling and aeration were the same as that mentioned at Section 2.2. At the end of incubation, the water phase containing SPS was decanted; SPS and water were separated by standing for 12 h. The denitrifying and nitrifying bacteria densities in the water phase, bed-sediment, and SPS samples were measured using MPN-PCR method. The CND rate was calculated according to the production of $^{15}N_2$, while nitrification rate was calculated according to the variation of NH_4^+-N concentration in the systems. To distinguish the contribution of SPS itself and agitation to the increased N loss through CND caused by the presence of SPS, another experiment set was carried out for systems containing bed-sediment and water (BS-WS) without agitation using samples collected from site AS. The control sets were conducted as the same as that mentioned at Section 2.2.

2.4. Incubation of bed sediment-SPS-water system with various nitrate concentration

To investigate the influencing mechanisms of SPS concentration on CND, the effect of initial NO_3^- concentration ($[NO_3^-]$) on denitrification was investigated by using samples collected from the site HYK. The 10-cm-deep sediment columns were constructed using the same method as Section 2.3, then 800 mL artificial overlying water containing 10, 6, 4.5, 3 and 1 mg L^{-1} NO_3^--N as KNO$_3$ were respectively added into each chamber. These concentrations are within the range of NO_3^- concentration detected in the Yellow River (Xia et al., 2002). Triplicate experiments were conducted for each incubation set. The SPS concentration in each column was set at 8 g L^{-1} by adjusting agitation rate, which

occurred in the temperate seasons (October–November and March–June) in the Yellow River. Then all the chambers were incubated at 25 °C. At pre-determined intervals (every two to four days), bed-sediment, SPS, and water samples were collected by using columnar samplers, and the samples were then put into tubes to separate sediment (including SPS and bed-sediment) and water phases by centrifuge; sediment and water samples were subsequently analyzed for the concentrations of N species. The denitrification rate was calculated according to the variation of $[NO_3^-]$ in the systems including SPS, bed-sediment, and water phases. The other experimental procedures were the same as that in Section 2.3. All the above mentioned experimental conditions are summarized in Table 2.

2.5. Chemical analysis

Water sample was filtrated through 0.45 μm filters (Millipore Corp. USA), and analyzed for NO_3^--N, NO_2^--N, and NH_4^+-N concentrations immediately. The NO_3^--N, NO_2^--N, and NH_4^+-N contents in sediment were analyzed after extraction with KCl solution (2 M). Dissolved nitrogen (NO_3^--N, NO_2^--N, and NH_4^+-N) concentrations were detected using an Autoanalyser-3 (Bran & Luebbe, France). Organic nitrogen contents in the sediment and water were measured after Kjeldahl digestion. Analytical reagents were used throughout the chemical analysis. The standard deviations for standards and replicate analysis were <4.4%, 2.8%, 5.4%, 5.0% for NH_4^+-N, NO_2^--N, NO_3^--N and organic nitrogen, respectively. The $^{15}N_2$ in gas samples was detected through using an isotopic ratio mass spectrometer (Thermo Delta V Advantage), in line with an automated gas PreCon unit. Nitrogen isotope ratios (including 29/28 and 30/28) of the samples were expressed as standard δ notation (‰) relative to atmospheric N_2. The standard deviation for standards and replicate analysis of the $δ^{15}N$ measurement was better than 0.2‰.

The SPS concentration in each water sample was obtained by filtering a certain amount of water through a Pall membrane (0.45 μm) and weighing the filter residue after drying at 60 °C for 7–8 h. A Laser Particle Sizer (Microtrac, S3500) was used to measure the size characteristics of SPS. A TOC analyzer (Shimadzu TOC-500) was used to detect the total organic carbon (TOC) in water and sediment samples. An oxygen meter

Table 2
Incubation experiment conditions.

Research purpose	System composition	$^{15}NH_4^+$-N (mg L^{-1})	NO_3^--N (mg L^{-1})	SPS concentration (g L^{-1})	Particle size of SPS (μm)
Occurrence of CND at SPS	SPS + water (samples from site AS)	5	0	0 1 2.5 8 15 20	Homogenized sediment
O$_2$ flux and profile around SPS particle	SPS + water (samples from site AS)	5 (NH_4^+-N)	0	20	<20 20–50 50–100 >100
Effect of SPS concentration on CND in BS-SPS-WS	Bed-sediment + SPS + water (samples from sites HYK, LM, AS, 37-Dock, and WZ)	5	0	0 1 2.5 8 15 20	Homogenized sediment
Effect of initial nitrate concentration on denitrification in BS-SPS-WS	Bed-sediment + SPS + water (samples from site HYK)	0	1 3 4.5 6 10	8	Homogenized sediment
CND in BS-WS	Bed-sediment + water (samples from site AS)	5	0	0	Homogenized sediment

(Mettler Toledo, SG9-FK2) was used to monitor dissolved oxygen concentration of water. Redox potential, temperature, and pH of water were detected using a pH meter (Mettler Toledo, SG23).

2.6. Biological and statistical analysis

To investigate the abundances of denitrifying and nitrifying bacteria in SPS particles, bed-sediment, and overlying water samples, DNA from the water and/or sediment were extracted using an Ultra Clean Soil DNA Isolation Kit (Mo-bio Laboratories, Inc., Carlsbad, CA, USA). The extract-ed DNA were stored at −20 °C until analysis by most-probable-number (MPN)-PCR (Cochran, 1950; Rotthauwe et al., 1997; Liu et al., 2003). The detailed procedures on MPN-PCR are shown in Supplementary Section S3.

SPSS 18.0 for windows (SPSS Inc., Chicago IL, USA) was used for all statistical analyses in this research, including correlation analysis, non-linear fitting, and variance analysis. The significance of correlation between each two variables was tested by calculating the Pearson correlation coefficient, and the significant differences among groups were tested with Duncan's multiple range test.

3. Results and discussion

3.1. Effect of SPS concentration on CND in oxic SPS-water system

3.1.1. Dependence of CND rate on SPS concentration

The presence of CND in SPS-water system (SPS-WS) was assessed by measuring the $^{15}N_2$-N production from a $^{15}NH_4^+$-N addition, which can only occur by $^{15}NO_3^-$ production through nitrification of $^{15}NH_4^+$-N followed by its reduction to $^{15}N_2$ during denitrification or anammox. According to our research (submitted to *Biogeochemistry*), the $^{15}N_2$ production from anammox was very low in SPS-water system of the Yellow River, thus the $^{15}N_2$ production was primarily from CND in the present research. The average CND rate, expressed as $^{15}N_2$-N production, followed a power function with SPS concentration, and jumped from 25 to 264 μg-N m^{-2} d^{-1} when the concentration of SPS was elevated from 0 to 20 g L^{-1} (Fig. 2A). Even a low concentration of SPS (1 g L^{-1}) resulted in an 8-fold increase in the $^{15}N_2$-N production relative to water without SPS. In addition, both nitrifying and denitrifying bacteria populations increased with increasing SPS concentration (Fig. 2B) as power functions respectively ($p < 0.05$), and they were positively correlated with the average CND rate (Fig. S1). This data suggest SPS was providing conditions for CND to occur.

3.1.2. Conditions provided by SPS for CND

The activity of SPS particle was investigated by determining the O_2 flux and dissolved O_2 (DO) around the particle. The observed high O_2 influx around SPS particles and decrease in DO concentrations (Figs. 3, S2 and S3) suggest that oxygen was being consumed near SPS particle surfaces by nitrification and/or microbial respiration. The DO concentration in the bulk solution was approximately 8.2 mg L^{-1} (100% air saturated), but it decreased to <53% O_2 saturation near the surface for particles with size <100 μm, and the decrease was the sharpest near the surface of particles. Similarly, maximum increases in the O_2 influx (−2.073 to −0.612 pmol cm^{-2} s^{-1}) occurred near particle surface regardless of particle size. Particles with diameters smaller than 20 μm had the largest overall increase in O_2 influx (Fig. S3); this is likely caused by the higher organic carbon content (%) and larger specific surface area of smaller particles compared with particles with larger sizes (Table S3). Despite differences in O_2 influxes among particles of different sizes, the above results indicate a gradient of oxic and low oxygen conditions exists within SPS particles with oxic conditions at the surface layer and low oxygen conditions near the center of particle. It infers that SPS particles can act as activated redox sites for microbial nitrification and denitrification because some bacteria can conduct denitrification under limited/low oxygen conditions. According to our previous research (Liu et al., 2013b), most of the denitrifying bacteria in the Yellow River are facultative bacteria and can conduct denitrification
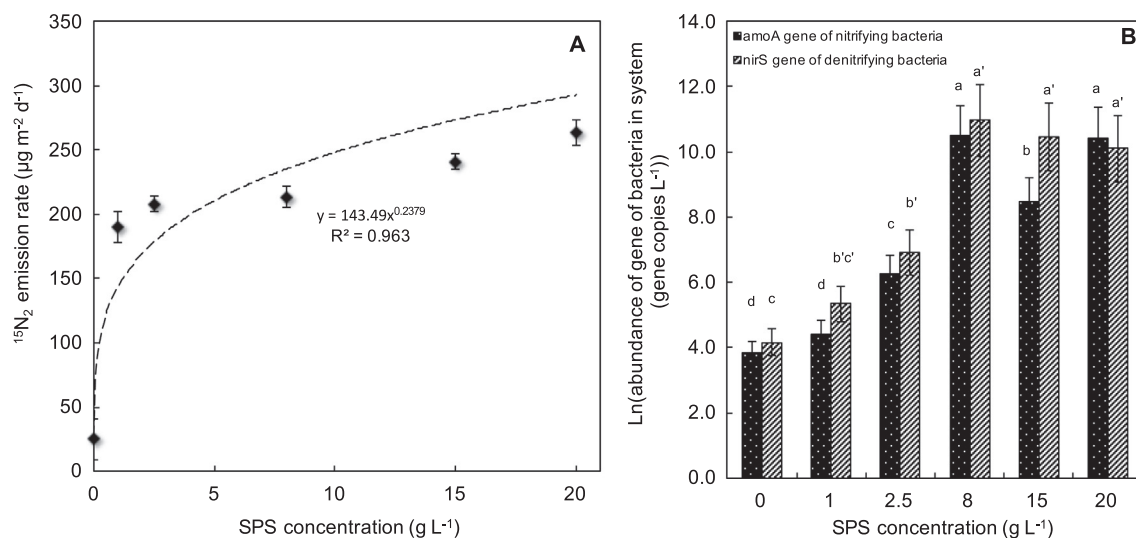
Fig. 2. Influence of suspended sediment concentration on $^{15}N_2$ emission (A), population of nitrifying and denitrifying bacteria (B) in suspended sediment-water system at the end of incubation (26 days). Data represent the average of three replicates ± SD; the a, b, c and a′, b′, c′ in (B) mean the significant differences among the 6 groups based on Duncan's multiple range test, respectively.
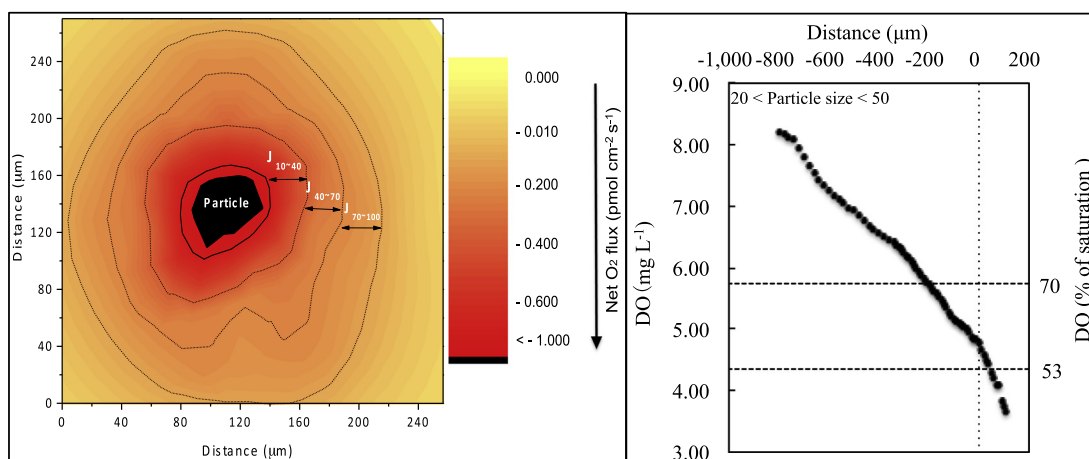
Fig. 3. Net O_2 flux (A) and O_2 gradient (B) around suspended sediment particles in relation to the distance from near the surface of SPS particle. Note: J indicates the flux (pmol cm^{-2} s^{-1}); negative values of net O_2 flux in (A) indicate net influxes; negative values of distance in (B) indicate the distance away from particle surface in bulk solution, and positive values of distance in (B) indicate the distance away from particle surface within particle. Oxygen levels of 53% and 70% air saturation represented the levels where facultative bacteria, which were identified as *Alcaligenes faecalis* and *Paracoccus denitrificans* on the SPS in the Yellow River, can conduct denitrification (Liu et al., 2013a,b).

under limited/low oxygen conditions (oxygen level <53% and <70% of the saturated O_2 concentration, respectively). Therefore, the presence of SPS in the Yellow River can provide microsite redox conditions needed for CND. In addition, because the SPS used in our incubation experiment had lower organic carbon contents than other rivers (Table S4), the SPS in other rivers might provide low/limited oxygen even anoxic micro-environments for denitrification.

Therefore, the mechanisms about the influence of SPS on CND in oxic waters can be analyzed as follows. The nitrifying bacteria distribute on the outer layer of particles and perform nitrification under high oxygen conditions, and the denitrifying bacteria reduced nitrate to N_2 at the deep layer of particles under low oxygen conditions. That is to say, firstly, the oxic conditions and NH_4^+-N adsorbed on the surface layer of suspended particles favor nitrification, and the nitrification rate rises with SPS concentration as a power function due to the fact that the percentage of NH_4^+-N sorbed on SPS increases with SPS concentration following a power function (Xia et al., 2009). Secondly, not only respiration by heterotrophic bacteria but nitrification at SPS particles lead to the presence of microsites with limited/low oxygen around/inside SPS particles, providing conditions for denitrification. The existence of both oxygen-limited microsites and denitrifying bacteria within the SPS particles promotes denitrification. These relationships between nitrification and denitrification at SPS particles lead to the occurrence of CND at SPS particles, as well as the accelerated CND rate with SPS concentration.

The positive correlation of nitrification with SPS concentration has been observed for river systems (Xia et al., 2009; Hsiao et al., 2014), and such a correlation has been reported in the relatively turbid region of estuaries with higher nitrification activities (Helder and De Vries, 1983; Owens, 1986; Berounsky and Nixon, 1993). In addition, although denitrification is most commonly observed in anoxic sediments, this process has also been reported for oxic environments where anoxic micro environments are thought to be associated with suspended particle surfaces and/or biofilms (Rao et al., 2008; Liu et al., 2013b; Reisinger et al., 2016). Furthermore, for the high-turbidity river mouth, the *amoA* and *nirS* genes abundances of the particle-associated (>3 μm) were found to be significantly higher than the free-living communities (0.2–3 μm) (Zhang et al., 2014). These research results
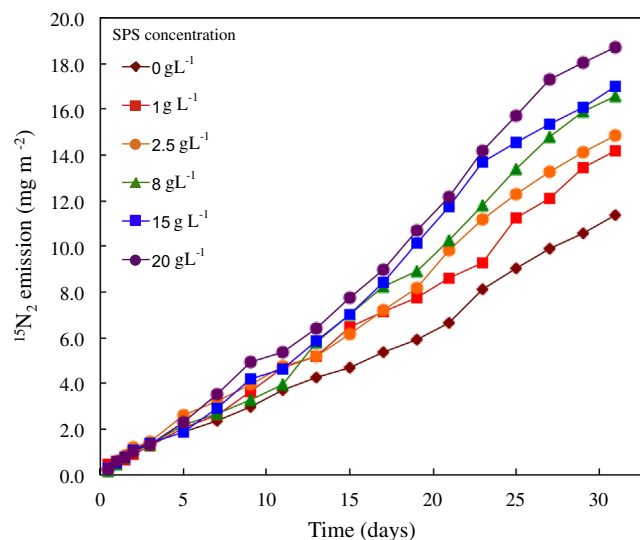
Fig. 4. Effect of suspended sediment concentration on the $^{15}N_2$ production from $^{15}NH_4^+$-N in bed sediment-suspended sediment-water system (BS-SPS-WS) for samples collected from site HYK of the Yellow River. Data represent the average of three replicates, and the standard deviation is <10%. Note: the effect of SPS concentration on $^{15}N_2$ production for samples from site AS, WZ, LM, 37-Dock is shown in Fig. S4.
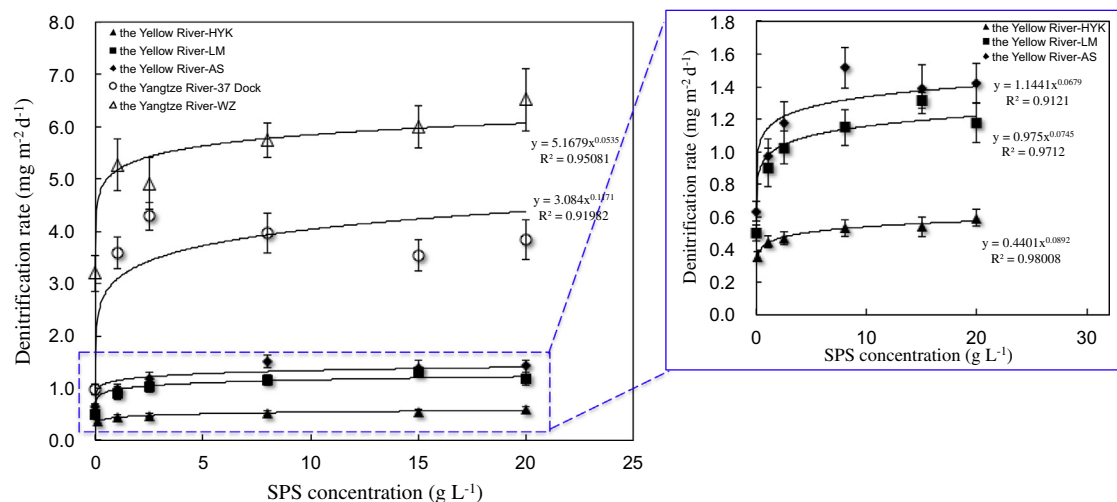
Fig. 5. Power functional relationship between suspended sediment concentration and production rate of $^{15}N_2$ from $^{15}NH_4^+$-N in bed sediment-suspended sediment-water system (BS-SPS-WS) for samples collected from different sites of the Yellow River and the Yangtze River, respectively. Data represent the average of three replicates ± SD.

suggest that the suspended particles and biofilms can promote both nitrification and denitrification in freshwater and seawater systems, which is probably due to the fact that the particles and biofilms can provide microsite redox conditions for both nitrification and denitrification.

3.2. Influence of SPS concentration on CND in bed sediment-SPS-water system

3.2.1. Increased $^{15}N_2$ production from $^{15}NH_4^+$ with SPS concentration

The production of $^{15}N_2$ produced by CND increased with incubation time and SPS concentration for the bed sediment-SPS-water system (BS-SPS-WS) using samples collected from five sites of the Yellow and Yangtze Rivers (Figs. 4 and S4). The average $^{15}N_2$ production rate increased dramatically with SPS concentration at low SPS concentrations and the increase tapered off at higher SPS concentrations. For the HYK sample, the $^{15}N_2$ production rate increased by 0.1 mg-N m^{-2} d^{-1} when SPS concentration increased from 0 to 1 g L^{-1}, but only increased by an additional 0.008 mg-N m^{-2} d^{-1} when SPS increased from 1 to 20 g L^{-1}.

The average $^{15}N_2$ production rate ($R_{15N2\text{-}production}$, mg-N m^{-2} d^{-1}) during incubation in BS-SPS-WS increased with SPS concentration ([SPS], g L^{-1}) as a power function for all of the five study sites (Fig. 5):

$$R_{15N2\text{-}production} = a \cdot [SPS]^b \qquad (1)$$

This indicates the universality of the relationship between N-loss rate and SPS concentration. As shown in Fig. S5, the constant a, reflecting the nitrogen loss rate with 1 g L^{-1} SPS, was positively related to the TOC content of SPS and the percentage of particles smaller than 20 μm ($p < 0.05$). The constant b, reflecting the dependence of N-loss on SPS concentration, was also positively related to the TOC content of SPS ($p < 0.05$). This was probably due to the fact that high TOC content favored the growth of heterotrophic denitrifying bacteria. Smaller particles might provide more favorable conditions for CND due to the sharper decrease of O_2 concentration near the particles and provided more sites for bacteria to grow due to larger specific surface areas. According to our previous research, the denitrification rate was negatively related to particle size of SPS in oxic waters (Jia et al., 2016). The enhancement of the N-loss rate by the presence of SPS differed among samples collected from various sites, indicating local biogeochemical conditions can control N-loss. For example, the sediments at site WZ of the Yangtze River that had the highest fine particle (<20 μm) percentage and TOC content among the five study sites also had the highest N-loss rate.

3.2.2. Influence of SPS concentration on nitrogen transformation

The presence of SPS accelerated the transformation of NH_4^+-N to NO_3^--N (Figs. 6 and 7). For the HYK sample, NH_4^+ concentration ([NH_4^+]) decreased nearly to zero by the 11th day in systems when SPS concentrations were between 8 and 20 g L^{-1}, while it remained over 1.5 mg L^{-1} in the system without SPS after 31 days of incubation. The average NH_4^+-N loss rate at the first nine days ascended with SPS concentration by a power function ($r = 0.921$, $p < 0.01$, Fig. 7). Correspondingly, the NO_3^- concentration ([NO_3^-]) increased and the $^{15}N_2$ evolved from each column along with the decrease in [NH_4^+] (Fig. 6), supporting the hypothesis of coupled nitrification-denitrification. However, a certain amount of NO_3^--N was accumulated in systems, which meant not all of the NO_3^--N produced from nitrification was denitrified immediately.

In the incubation experiments of bed sediment-SPS-water system, ammonification, anammox, dissimilatory nitrate reduction to ammonium (DNRA), and inorganic nitrogen uptake may occur simultaneously in addition to nitrification and denitrification processes. Overall, approximately 1.8%, 3.6%, 6.4%, 12%, and 20% of the added ^{15}N in the form of NH_4^+-N has been transformed into N_2 after incubation for 31 d for the bed sediment-SPS-water system containing 20 g L^{-1} SPS collected from HYK, LM, AS, 37 Dock, and WZ Stations, respectively. In detail, taking the HYK for example (Table S3), approximately 1.80% and 71.8% of the added ^{15}N in the form of NH_4^+-N has been transformed into N_2 and NO_3^- for the incubations with 20 g L^{-1} SPS, respectively; approximately 5.09% remained as NH_4^+ and 21.3% assimilated by organisms based on the mass balance of added NH_4^+-N.

The variation of NH_4^+ concentration was affected by ammonification, nitrification, anammox, DNRA, and its uptake by heterotrophic organisms. As shown in Fig. 6 for the HYK sample, NH_4^+ concentration increased during the first three days of the incubation systems with SPS concentration <2.5 g L^{-1}; this might be ascribed to the ammonification. After that, NH_4^+ concentration decreased significantly, suggesting that nitrification,
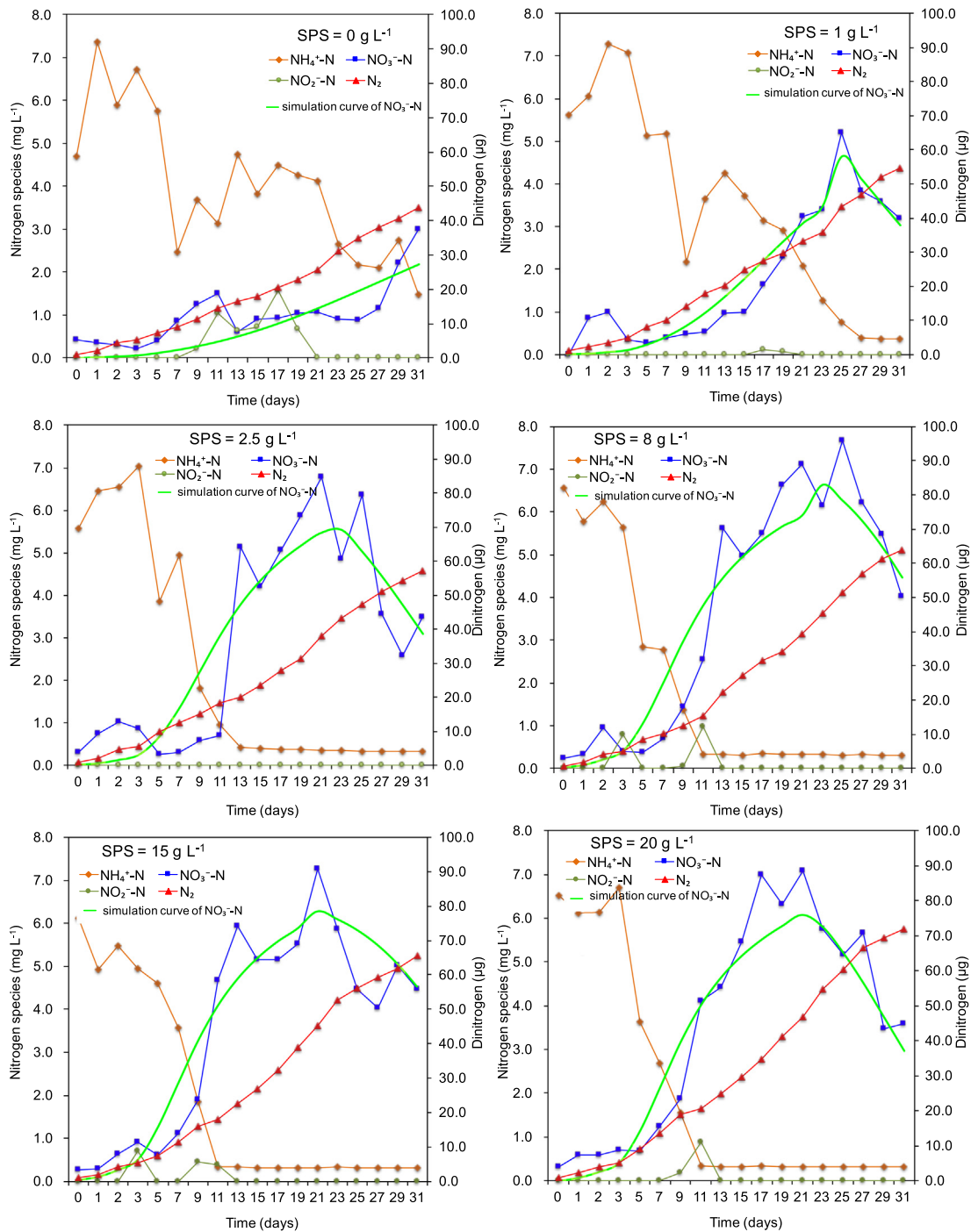
Fig. 6. Variations of NH_4^+, NO_3^-, NO_2^-, and N_2 in bed sediment-suspended sediment-water system (BS-SPS-WS) containing different concentrations of suspended sediment for samples collected from site HYK of the Yellow River. Data represent the average of three replicates, and the standard deviation is <0%.

anammox, and uptake by heterotrophic organisms controlled the variation of NH_4^+. Although Lansdown et al. (2016) found that anammox can represent an important nitrogen loss pathway in permeable river sediments, some researchers reported that the contribution of anammox process, in the riverine sediments, to the N-loss was approximately 10% (Dale et al., 2009; Wang et al., 2012; Zhu et al., 2015). The anammox process might be less significant than nitrification in the present research because the sediment was different from that studied by Lansdown et al. In addition, the fraction of NH_4^+ transformed to NO_3^- (55.6%–89.5%) was much higher than the assimilation (3.71%–28.9%) (Table S5). The variation of NO_3^- concentration would be affected by nitrification, DNRA, and denitrification. DNRA has been shown as significant in many organic rich sediments and for instance during oxic-anoxic oscillations (Abril et al., 2010). As <23% of the added NH_4^+ remained as NH_4^+, the DNRA must be much less significant than nitrification in the present research. In addition, the TOC content of the sediment sample was low (Table 1), therefore, the DNRA might be not significant in the incubations of the present research. However, SPS might provide oxic-anoxic oscillations for DNRA in other rivers, and more research should be conducted in this regard.

According to the above analysis, the variations of NH_4^+ and NO_3^- in the incubation systems resulted from several processes. However, the transformation of added NH_4^+ was mainly controlled by nitrification and denitrification. Therefore, the processes were simplified as nitrification and
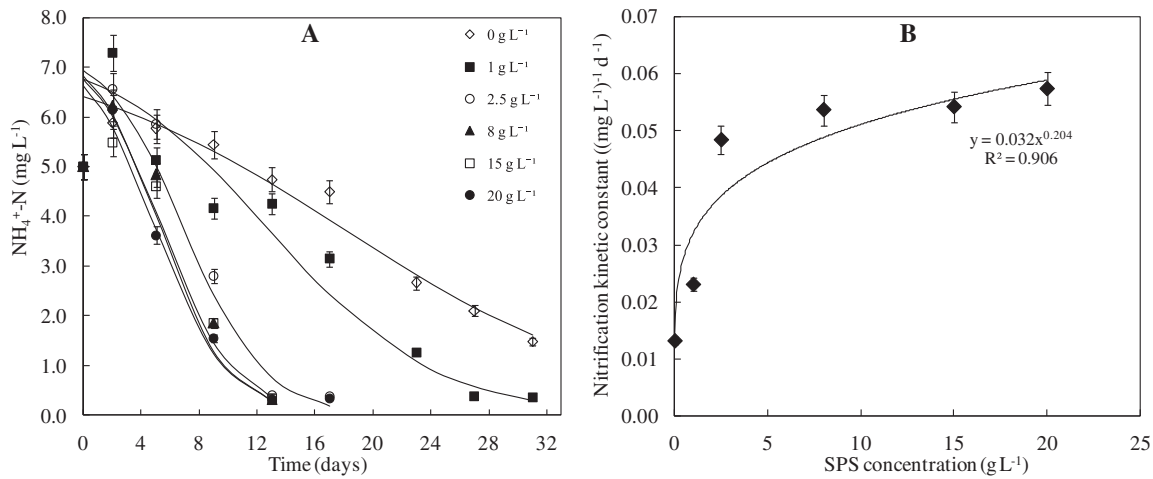
Fig. 7. Variation of NH_4^+-N concentration with time and its fitting with the Logistic model (A), and the relation of nitrification rate constants with suspended sediment concentration (B) in bed sediment-suspended sediment-water system (BS-SPS-WS) for samples collected from site HYK. Data represent the average of three replicates ± SD.

denitrification to study the nitrogen transformation kinetics of the present research. The following logistic model was used to analyze NH_4^+-N variation during nitrification:

$$\left(-\frac{dS_{NH_4^+}}{dt}\right)_{\text{nitrification}} = \frac{\mu_{max\text{-nitrifier}}S_{NH_4^+}\left(S_{NH_4^+0} + X_{0\text{-nitrifier}} - S_{NH_4^+}\right)}{k_{s\text{-nitrifier}}} \tag{2}$$

the integral form of Eq. (2) is:

$$S_{NH_4^+} = \frac{S_{NH_4^+0} + X_{0\text{-nitrifier}}}{1 + \left(X_{0\text{-nitrifier}}/S_{NH_4^+0}\right) \cdot e^{k_{\text{nitrification}}\left(S_{NH_4^+0} + X_{0\text{-nitrifier}}\right)t}} \tag{3}$$

where $S_{NH_4^+}$ represents the $[NH_4^+]$ at time t (mg L^{-1}); $S_{NH_4^+0}$ represents the $[NH_4^+]$ in the beginning (mg L^{-1}); $X_{0\text{-nitrifier}}$ represents the bacterial population quota in the beginning (mg L^{-1}); $k_{\text{nitrification}}$ represents the nitrification rate constant (d^{-1} (mg L^{-1})$^{-1}$), $k_{\text{nitrification}} = \mu_{max\text{-nitrifier}}/K_{s\text{-nitrifier}}$; $\mu_{max\text{-nitrifier}}$ represents the maximum specific growth rate of nitrifying bacteria (d^{-1}); $K_{s\text{-nitrifier}}$ represents the half-saturation growth constant for nitrifying bacteria (mg L^{-1}). The NH_4^+-N variation in systems containing various SPS concentrations fit well with the Logistic model shown in Eq. (2) ($p < 0.01$), and the nitrification rate constant ($k_{\text{nitrification}}$) increased with SPS concentration conforming to a power function ($p < 0.01$, Fig. 7 and Table 3).

The variation of nitrate during CND depends on relative nitrification and denitrification rates, and the latter was described by the Monod kinetics:

$$\frac{dS_{NO_3^-}}{dt} = \frac{d\left(S_{NH_4^+0} - S_{NH_4^+}\right)}{dt} - \left(\frac{\mu_{max\text{-denitrifier}}S_{NO_3^-}\left(S_{NO_3^-0} + X_{0\text{-denitrifier}} - S_{NO_3^-}\right)}{\left(K_{s\text{-denitrifier}} + S_{NO_3^-}\right)}\right) \tag{4}$$

where $S_{NO_3^-}$ represents the $[NO_3^-]$ at time t (mg L^{-1}); $S_{NO_3^-0}$ represents the initial $[NO_3^-]$ (mg L^{-1}); $\mu_{max\text{-denitrifier}}$ represents the maximum specific growth rate of denitrifying bacteria (d^{-1}); $X_{0\text{-denitrifier}}$ represents the denitrifying bacterial population quota in the beginning (mg L^{-1}); $K_{s\text{-denitrifier}}$ represents the half-saturation growth constant for denitrifying bacteria (mg L$_{-1}$). As shown in Fig. 6, the kinetics of nitrate in system could be divided into two stages. At the first stage, $[NO_3^-]$ increased with time; the denitrifying bacteria was much higher than $[NO_3^-]$ at time zero ($X_{0\text{-denitrifier}} \gg S_{NO_3^-0}$) and the $K_{s\text{-denitrifier}}$ was much higher than $[NO_3^-]$ as well ($K_{s\text{-denitrifier}} \gg S_{NO3}$), accordingly Eq. (4) could be simplified as Eq. (4-1). At the second stage, $[NO_3^-]$ decreased with time while $[NH_4^+]$ kept constant at ~0.3 mg L^{-1} (*i.e.*, $\frac{d(S_{NH_4^+0} - S_{NH_4^+})}{dt} = 0$); $K_{s\text{-denitrifier}}$ was much higher than nitrate concentration

Table 3
Nitrification and denitrification rate constants in bed sediment-SPS-water systems for samples collected from site HYK of the Yellow River.

SPS concentration (g L^{-1})	Nitrification rate constant ($k_{\text{nitrification}}$, (mg L^{-1})$^{-1}$ d^{-1})	Denitrification rate constant in the first stage ($k_{\text{denitrification-1}}$, d^{-1})	Denitrification rate constant in the second stage ($k_{\text{denitrification-2}}$, (mgL^{-1})$^{-1}$ d^{-1})
0	0.013	0.015	/
1	0.023	0.034	0.0203
2.5	0.048	0.063	0.0278
8	0.053	0.075	0.0281
15	0.054	0.081	0.0298
20	0.057	0.079	0.0290
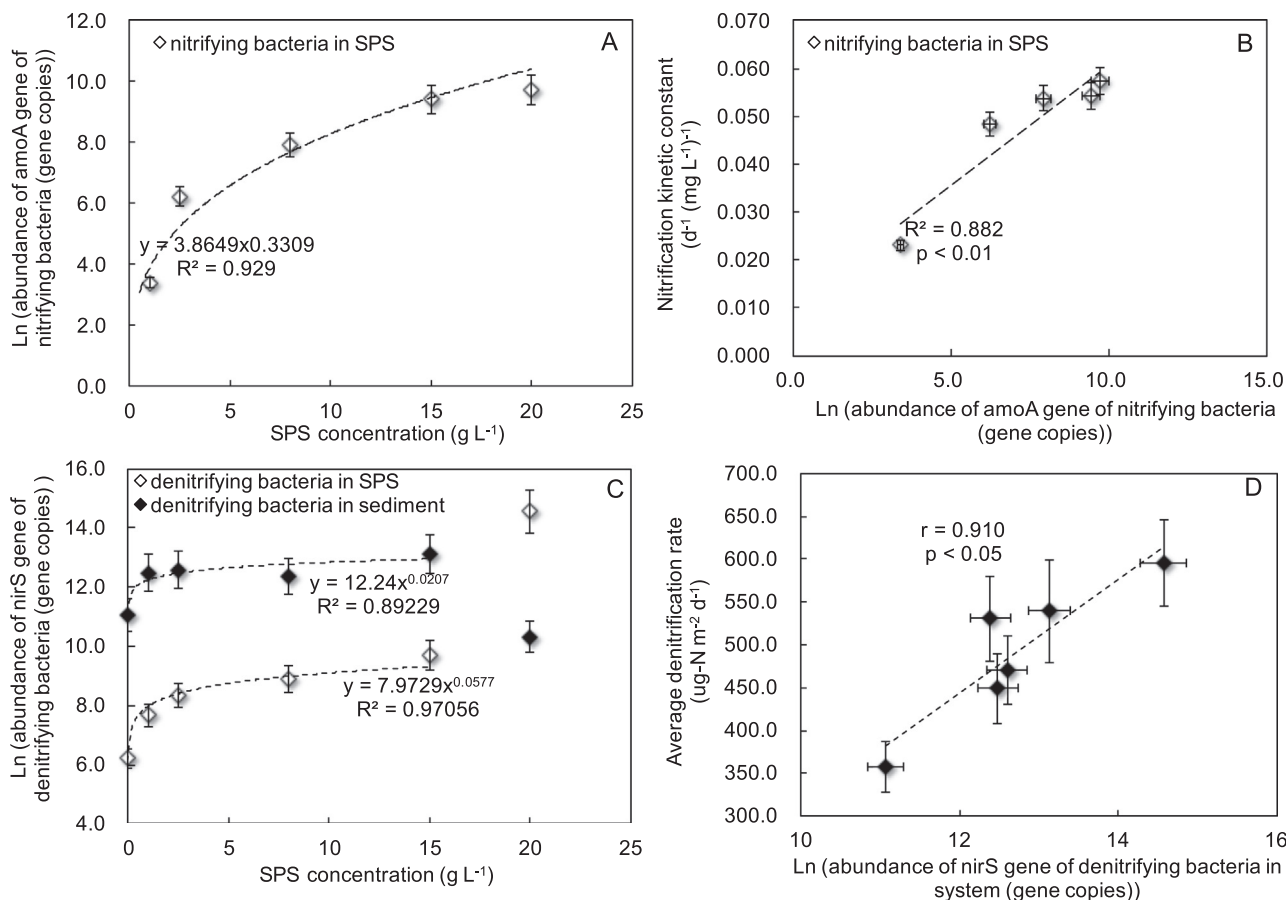
Fig. 8. Relationship between SPS concentration and nitrifying bacteria population (A), between nitrification rate constant and nitrifying bacteria population (B), between suspended sediment concentration and denitrifying bacteria population (C), and between average denitrification rate and denitrifying bacteria population (D) in bed sediment-suspended sediment-water system (BS-SPS-WS) for samples collected from site HYK.

($K_{\text{s-denitrifier}} \gg S_{\text{NO3}}$), accordingly Eq. (4) could be simplified as Eq. (4-2) as follows:

$$\frac{dS_{NO_3^-}}{dt} = \begin{cases} \dfrac{d\left(S_{NH_4^+0}-S_{NH_4^+}\right)}{dt} - \dfrac{\mu_{\text{max-denitrifier}} \cdot S_{NO_3^-} \cdot X_{0\text{-denitrifier}}}{K_{\text{s-denitrifier}}} & \text{(First Stage)} \quad (4\text{-}1) \\[3mm] \dfrac{\mu_{\text{max-denitrifier}} \cdot S_{NO_3^-}\left(S_{NO_3^-0} + X_{0\text{-denitrifier}} - S_{NO_3^-}\right)}{K_{\text{s-denitrifier}}} & \text{(Second Stage)} \quad (4\text{-}2) \end{cases}$$

the integral forms of Eqs. (4-1) and (4-2) are:

$$S_{NO_3^-} = \begin{cases} \dfrac{S_{NH_4^+0} + X_{0\text{-nitrifier}}}{1 + \left(X_{0\text{-nitrifier}}/S_{NH_4^+0}\right) \cdot e^{k_{\text{nitrification}}\left(S_{NH_4^+0}+X_{0\text{-nitrifier}}\right)t}} \cdot \left(1 - e^{k_{\text{denitrification-1}}t}\right) & \text{(First Stage)} \quad (5\text{-}1) \\[4mm] \dfrac{S_{NO_3^-0} + X_{0\text{-denitrifier}}}{1 + \left(X_{0\text{-denitrifier}}/S_{NO_3^-0}\right) \cdot e^{k_{\text{denitrification-2}}\left(S_{NO_3^-0}+X_{0\text{-denitrifier}}\right)t}} & \text{(Second Stage)} \quad (5\text{-}2) \end{cases}$$

where $k_{\text{denitrification-1}}$ is the denitrification rate constant during the first stage (d^{-1}), $k_{\text{denitrification-1}} = \frac{\mu_{\text{max-denitrifier}} \cdot X_{0\text{-denitrifier}}}{K_{\text{s-denitrifier}}}$; $k_{\text{denitrification-2}}$ is the denitrification rate constant during the second stage (d^{-1} $(mg\ L^{-1})^{-1}$), $k_{\text{denitrification-2}} = \mu_{\text{max-denitrifier}}/K_{\text{s-denitrifier}}$.

Based on the variations of [NO_3^-] shown in Fig. 6, the kinetics of nitrate fit the Eqs. (5-1) and (5-2) very well ($p < 0.01$). According to the results shown in Table 3, the denitrification rate constant ($K_{\text{denitrification-1}}$) ascended with SPS concentration conforming to a power function during the first stage (Fig. S6), coinciding with the relationship between nitrification rate constant ($k_{\text{nitrification}}$) and SPS concentration as mentioned before. It implied that the denitrification rate might be tightly related to nitrate available produced by nitrification. For the system containing 0 g L^{-1} SPS, the second stage did not occur obviously; the denitrification rate constant ($k_{\text{denitrification-2}}$) in systems containing 1, 2.5, 8, 15, and 20 g L^{-1} SPS also ascended with SPS concentration conforming to a power function ($R^2 = 0.72$) during the second stage, indicating the enhanced effect of SPS on denitrification.
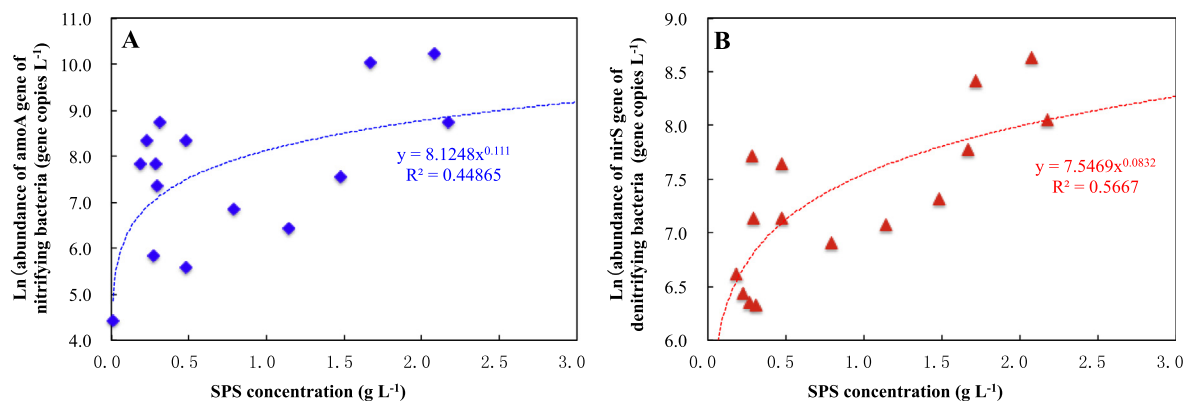
Fig. 9. The *in-situ* nitrifying and denitrifying bacteria population in water samples (containing suspended sediment) collected from the Yellow River (15 sites).

3.3. Mechanisms about the influence of SPS on CND in bed sediment-SPS-water system

3.3.1. Influence of SPS concentration on bacterial abundances

The SPS's nitrifying bacteria populations increased with SPS concentration also following a power function ($R^2 = 0.93$, Fig. 8A), which was similar to the nitrification rate dependence on the SPS concentration. Nitrification rates were positively correlated to nitrifying bacteria populations in SPS ($p < 0.01$, Fig. 8B). The nitrifying bacteria population in the bed sediment, however, was smaller than that in the SPS and did not show an obvious relationship with nitrification rate (Fig. S7). This implies that NH_4^+-N loss in the system was mainly caused by nitrification occurring on SPS, not in the bed-sediments.

For both SPS and bed-sediment, the denitrifying bacteria population increased with SPS concentration as a power function (Fig. 8C). When SPS concentration was elevated from 15 to 20 g L^{-1}, the denitrifying bacteria in SPS jumped from 1.6×10^4 to 2.1×10^6 gene copies while the bed-sediment decreased from 4.9×10^5 to 3.0×10^4 gene copies. This might have been caused by abrupt increase in oxygen-limited microsites at SPS phase due to cohesions of SPS particles and the increased oxygen diffusion into the sediment caused by increasing agitation rate. Overall, when SPS concentration increased from 0 to 20 g L^{-1}, the total denitrifying bacteria in system (bacteria in SPS plus that in bed-sediment) increased with SPS concentration and was positively related to denitrification rate ($p < 0.05$, Fig. 8D). Therefore, it suggests that denitrification in systems was related to denitrifying bacteria in not only SPS but also bed-sediment.

3.3.2. Influence of SPS concentration on denitrification in bed-sediment

Some of the NO_3^- produced by nitrifying bacteria on SPS was subsequently reduced to N_2 in oxygen-limited microsites of SPS and the remaining NO_3^- diffused into bed-sediment where it was denitrified. Therefore, the NO_3^- produced by nitrification at SPS would exert influences on the denitrification process occurring not only in SPS but also in bed-sediment phases. As shown in Fig. S8, the average removal rate of NO_3^- (including denitrification and other process) increased linearly with initial NO_3^- concentration ($p < 0.01$, Supplementary Section S4) in bed sediment-SPS-water system, suggesting that denitrification rate was influenced by nitrate availability. According to the results shown in Fig. S9, the average CND rates were 248, 634, 1515 µg m^{-2} d^{-1} in systems containing only 8 g L^{-1} SPS, containing bed-sediment but without SPS, containing both 8 g L^{-1} SPS and bed-sediment, respectively. Based on our estimations (Supplementary Section S5), compared to the system with bed-sediment covered by static water, roughly 28% of the increased N-loss in bed sediment-SPS-water system was ascribed to N-loss at SPS and 72% to N-loss in bed-sediment accelerated by elevated nitrate supply produced by overlying-water nitrification which was enhanced by the presence of SPS. Because agitation, simulating the river flow and causing the presence of SPS, would pose effects on the diffusion of nitrate from water to bed-sediment, the increased nitrate supply in bed-sediment was also caused by the agitation conditions in addition to the presence of SPS itself which accelerated the production of nitrate. Since SPS concentration also depends on hydrodynamic conditions including river flow velocity in natural rivers (Xia et al., 2016), the results obtained under different agitation rates in this study can reflect the effect of SPS concentration on N-loss from natural rivers.

3.4. The in-situ nitrifying and denitrifying bacteria abundances in the Yellow River

Both the *in-situ* nitrifying and denitrifying bacteria populations in water (including aqueous and SPS phases) in the Yellow River rose with SPS concentration following a power function (Fig. 9, despite approaching linearity, a power function still fit these data better), which was in accordance with the relationship between bacteria population and SPS concentration observed in the lab experiments. This implies that the N-loss rate in natural rivers will increase with SPS concentration as we have observed in the incubation experiments.

3.5. Importance of SPS to N loss from river systems

As the N-loss in the incubation systems might also be caused by anammox processes in addition to denitrification, the N-loss caused by coupled nitrification-denitrification might be lower than the emission of $^{15}N_2$ observed in the incubation experiments of the present research. However, our data show that SPS enhances the nitrification and denitrification processes as well as N-loss from rivers. NH_4^+ and NO_3^- are the main inorganic nitrogen species in the Yellow River and Yangtze River, and they mainly come from nitrogenous fertilizer application and wastewater discharge (Xia et al., 2002; Li et al., 2010; Liu et al., 2013a), with a relatively low atmospheric deposition contribution. This is significantly different from the ocean where up to one third of the external nitrogen supply comes from the atmospheric anthropogenic fixed nitrogen (Duce et al., 2008). NH_4^+ and NO_3^- can be removed through CND, anammox, and denitrification processes in natural rivers. In the present research, although the initial NH_4^+

concentration was much higher while NO_3^- concentration was much lower than their concentrations in natural rivers, respectively, the results showed that the SPS can enhance CND as well as N-loss from rivers if N exists as NH_4^+. In addition, our previous study showed that if N exists as NO_3^-, N loss through denitrification increases with the SPS concentration as well (Liu et al., 2013b). Therefore, according to the results of this study and our previous study, it is suggested that the total N-loss in the Yellow River and the Yangtze River will increase with the SPS concentration. However, more research should be carried out to study the effect of SPS on N-loss in natural river systems.

Based on the $^{15}N_2$ emission rate in the SPS-water system obtained in this study, the CND rate is estimated at 730 kg-N/km^2·yr $(\frac{200 \text{ mg/m}^2 \cdot d \times 365 d \times 200 cm}{20 cm} = 730 \text{ kg N/km}^2 \cdot \text{yr})$ for rivers with 1 g L^{-1} SPS and a depth of 2 m. Previous study reported that denitrification occurring in river networks (including continental shelf, terrestrial, oceanic oxygen minimum zones, groundwater, rivers, lakes, and estuaries globally) has an average denitrification rate of 0 to 2173 kg-N/km^2·yr (Seitzinger et al., 2006). This is at comparable scales to the N-loss caused by CND occurring on SPS in the present study, suggesting that CND on SPS cannot be neglected in river N removal.

We defined the increased proportion of N-loss ($\Delta\%_{Nloss}$) caused by SPS as follows:

$$\Delta\%_{Nloss} = \frac{N_{loss} \text{ in BS-SPS-WS containing SPS-}N_{loss} \text{ in BS-WS without SPS}}{N_{loss} \text{ in BS-WS without SPS}} \times 100 \tag{6}$$

If SPS concentration was assumed to be 1 g L^{-1}, the $\Delta\%_{Nloss}$ in the samples collected from the HYK, LM, AS, WZ, and 37-Dock location were 25%, 53%, 53%, 80%, and 122%, respectively; they were positively related to the TOC of SPS (Fig. S10). The above results indicate that the accelerated effect of SPS on N-loss was impacted by both concentration and properties of SPS. In addition, according to the above results, the increased proportion of N loss caused by SPS reached 100% when SPS concentration increased to 1 g L^{-1} in the Yangtze River (TOC $\approx$ 0.64%). Approximately 46% of the rivers around the world has SPS concentration higher than 1 g L^{-1} (Xia et al., 2016), and the TOC content in most of these rivers are higher than that in the Yangtze River (Table S4), thus the nitrogen loss in these rivers might increase at least by one time due to the presence of SPS.

The importance of water column processes becomes increasingly remarkable with the increase of stream size according to the river continuum concept (Vannote et al., 1980), and Reisinger et al. (2015) also reported that the water column nutrient uptake including assimilation and dissimilatory transformation increase with stream size. Therefore, for the large rivers of the world, where the interaction between the water column and the bed sediment is limited, coupled nitrification-denitrification and other nitrogen transformation processes in the overlying water containing SPS will act as a crucial role in nitrogen loss in river systems. Traditional frameworks of global N cycle have not considered coupled nitrification-denitrification and other processes occurring on SPS, leading to an underestimation of N-loss from rivers, especially for the large rivers. The observation of the present research is consistent with recent research that the estimated global N budget is out of balance, with inputs exceeding losses (Galloway et al., 2004; Schlesinger, 2009). Therefore, the enhanced effect of SPS on N-loss from rivers need to be factored into the new generation model of N cycle. Because spatio-temporal and vertical variations in SPS concentration and composition exist for each river (Bouchez et al., 2011a, 2011b; Xia et al., 2016), more research should be conducted to estimate the contribution of water column containing SPS to N-loss in rivers by considering the SPS concentration and composition as well as other environmental conditions and climatic factors including temperature. In addition, the linkage between SPS and emission of N_2O, an important greenhouse gas produced by nitrification/denitrification, should be examined to determine the role of SPS in nitrogen cycle under the context of climate change.

4. Conclusion

Taking the Yellow and Yangtze Rivers as examples, this study demonstrates that SPS, a major component of rivers, is a hot spot for both nitrification and denitrification through simulation experiments and *in-situ* investigation. CND could occur on SPS in oxic waters because of the presence of oxic and anoxic/low oxygen microsites around SPS; the nitrogen loss rate (R_{N-loss}) increased with SPS concentration ($[SPS]$) as a power function ($R_{N-loss} = a * [SPS]^b$). The influencing mechanisms of SPS on CND rate have been analyzed; the nitrifying and denitrifying bacteria population was elevated with SPS concentration conforming to a power function for both the lab simulation experiments and *in-situ* investigation of the Yellow River. This study suggests that 1 g L^{-1} SPS will lead to an enhancement in nitrogen loss by approximately 25–120% in the Yellow and Yangtze Rivers, and the enhancement increases with organic carbon content (TOC) of SPS. Thus N-loss from rivers in previous studies might be underestimated due to non-consideration of the presence of SPS; this may partially compensate for the current disequilibrium between N inputs and N sinks. The future N research regarding SPS needs to aim at estimating the role of SPS more accurately by considering other nitrogen transformation processes, and the SPS concentration and composition as well as other environmental conditions.

Acknowledgements

Appendix A. Supplementary data

Supplementary data to this article can be found online at http://dx.doi.org/10.1016/j.scitotenv.2016.10.181.

References

Abril, G., Commarieu, M.-V., Etcheber, H., Deborde, J., Deflandre, B., Živađinović, M.K., Chaillou, G., Anschutz, P., 2010. In vitro simulation of oxic/suboxic diagenesis in an estuarine fluid mud subjected to redox oscillations. Estuar. Coast. Shelf Sci. 88, 279–291.

Abril, G., Riou, S., Etcheber, H., Frankignoulle, M., De Wit, R., Middelburg, J., 2000. Transient, tidal time-scale, nitrogen transformations in an estuarine turbidity maximum—fluid mud system (the Gironde, south-west France). Estuar. Coast. Shelf Sci. 50, 703–715.

Berounsky, V.M., Nixon, S.W., 1993. Rates of nitrification along an estuarine gradient in Narragansett Bay. Estuaries 16, 718–730.

Bianchi, M., Marty, D., Teyssie, J.L., Fowler, S.W., 1992. Strictly aerobic and anaerobic-bacteria associated with sinking particulate matter and zooplankton fecal pellets. Mar. Ecol. Prog. Ser. 88, 55–60.

Billi, P., Ali, O.E., 2010. Sediment transport of the Blue Nile at Khartoum. Quatern. Int. 226, 12–22.

Bouchez, J., Lupker, M., Gaillardet, J., France-Lanord, C., Maurice, L., 2011a. How important is it to integrate riverine suspended sediment chemical composition with depth? Clues from Amazon River depth-profiles. Geochim. Cosmochim. Acta 75, 6955–6970.

Bouchez, J., Métivier, F., Lupker, M., Maurice, L., Perez, M., Gaillardet, J., France Lanord, C., 2011b. Prediction of depth-integrated fluxes of suspended sediment in the Amazon River: particle aggregation as a complicating factor. Hydrol. Process. 25, 778–794.

Boyer, E.W., Howarth, R.W., Galloway, J.N., Dentener, F.J., Green, P.A., Vörösmarty, C.J., 2006. Riverine nitrogen export from the continents to the coasts. Glob. Biogeochem. Cycle 20, 1–91.

Changjiang Water Resources Committee, 2014. Changjiang Sediment Bulletin. Ministry of Water Resources, Wuhan 430012, China.

Cochran, W.G., 1950. Estimation of bacterial densities by means of the most probable number. Biometrics 6, 105–116.

Dale, O.R., Tobias, C.R., Song, B., 2009. Biogeographical distribution of diverse anaerobic ammonium oxidizing (anammox) bacteria in Cape Fear River estuary. Environ. Microbiol. 11, 1194–1207.

Diaz, R.J., Rosenberg, R., 2008. Spreading dead zones and consequences for marine ecosystems. Science 321, 926–929.

Donner, S.D., Kucharik, C.J., 2008. Corn-based ethanol production compromises goal of reducing nitrogen export by the Mississippi River. P. Natl. Acad. Sci. USA 105, 4513–4518.

Duce, R.A., LaRoche, J., Altieri, K., et al., 2008. Impacts of atmospheric anthropogenic nitrogen on the open ocean. Science 320, 893–897.

Falkowski, P.G., Fenchel, T., Delong, E.F., 2008. The microbial engines that drive Earth's biogeochemical cycles. Science 320, 1034–1039.

Galloway, J.N., 1998. The global nitrogen cycle: changes and consequences. Environ. Pollut. 102, 15–24.

Galloway, J.N., Dentener, F.J., Capone, D.G., Boyer, E.W., Howarth, R.W., Seitzinger, S.P., Asner, G.P., Cleveland, C.C., Green, P.A., Holland, E.A., Karl, D.M., Michaels, A.F., Porter, J.H., Townsend, A.R., Vorosmarty, C.J., 2004. Nitrogen cycles: past, present, and future. Biogeochemistry 70, 153–226.

Gruber, N., Galloway, J.N., 2008. An earth-system perspective of the global nitrogen cycle. Nature 451, 293–296.

Helder, W., De Vries, R., 1983. Estuarine nitrite maxima and nitrifying bacteria (Ems-Dollard estuary). Neth. J. Sea Res. 17, 1–18.

Hsiao, S.S.Y., Hsu, T.C., Liu, J.W., Xie, X., Zhang, Y., Lin, J., Wang, H., Yang, J.Y.T., Hsu, S.C., Dai, M., Kao, S.J., 2014. Nitrification and its oxygen consumption along the turbid Chang Jiang River plume. Biogeosciences 11, 2083–2098.

Jaffe, L.F., Nuccitelli, R., 1974. An ultrasensitive vibrating probe for measuring steady extracellular currents. J. Cell Biol. 63, 614–628.

Jia, Z.M., Liu, T., Xia, X.H., Xia, N., 2016. Effect of particle size and composition of suspended sediment on denitrification in river water. Sci. Total Environ. 541, 934–940.

Johannsen, A., Dähnke, K., Emeis, K., 2008. Isotopic composition of nitrate in five German rivers discharging into the North Sea. Org. Geochem. 39, 1678–1689.

Lamontag, R., Swinnert, J., Linnenbo, V., Smith, W.D., 1973. Methane concentrations in various marine environments. J. Geophys. Res. 78, 5317–5324.

Lansdown, K., McKew, B.A., Whitby, C., Heppell, C.M., Dumbrell, A.J., Binley, A., et al., 2016. Importance and controls of anaerobic ammonium oxidation influenced by riverbed geology. Nat. Geosci. 9, 357–360.

Lenihan, H.S., Peterson, C.H., 1998. How habitat degradation through fishery disturbance enhances impacts of hypoxia on oyster reefs. Ecol. Appl. 8, 128–140.

Li, S.L., Liu, C.Q., Li, J., Liu, X., Chetalat, B., Wang, B., Wang, F., 2010. Assessment of the sources of nitrate in the Changjiang River, China using a nitrogen and oxygen isotopic approach. Environ. Sci. Technol. 44, 1573–1578.

Liu, T., Wang, F., Michalski, G., Xia, X., Liu, S., 2013a. Using ^{15}N, ^{17}O, and ^{18}O to determine nitrate sources in the Yellow River, China. Environ. Sci. Technol. 47, 13412–13421.

Liu, T., Xia, X.H., Liu, S.D., Mou, X.L., Qiu, Y.W., 2013b. Acceleration of denitrification in turbid rivers due to denitrification occurring on suspended sediment in oxic waters. Environ. Sci. Technol. 47, 4053–4061.

Liu, X.D., Tiquia, S.M., Holguin, G., Wu, L.Y., Nold, S.C., Devol, A.H., Luo, K., Palumbo, A.V., Tiedje, J.M., Zhou, J.Z., 2003. Molecular diversity of denitrifying genes in continental margin sediments within the oxygen-deficient zone off the Pacific coast of Mexico. Appl. Environ. Microb. 69, 3549–3560.

Mallin, M.A., Johnson, V.L., Ensign, S.H., MacPherson, T.A., 2006. Factors contributing to hypoxia in rivers, lakes, and streams. Limnol. Oceanogr. 51, 690–701.

Michotey, V., Bonin, P., 1997. Evidence for anaerobic bacterial processes in the water column: denitrification and dissimilatory nitrate ammonification in the northwestern Mediterranean sea. Mar. Ecol. Prog. Ser. 160, 47–56.

Mulder, T., Syvitski, J.P.M., 1995. Turbidity currents generated at river mouths during exceptional discharges to the world oceans. J. Geol. 103, 285–299.

Mulholland, P.J., Helton, A.M., Poole, G.C., Hall, R.O., Hamilton, S.K., Peterson, B.J., Tank, J.L., Ashkenas, L.R., Cooper, L.W., Dahm, C.N., 2008. Stream denitrification across biomes and its response to anthropogenic nitrate loading. Nature 452, 202–205.

O'Connor, B.L., Hondzo, M., 2007. Enhancement and inhibition of denitrification by fluid-flow and dissolved oxygen flux to stream sediments. Environ. Sci. Technol. 42, 119–125.

Owens, N.J., 1986. Estuarine nitrification: a naturally occurring fluidized bed reaction? Estuar. Coast. Shelf S. 22, 31–44.

Pina-Ochoa, E., Álvarez-Cobelas, M., 2006. Denitrification in aquatic environments: a cross-system analysis. Biogeochemistry 81, 111–130.

Rabalais, N.N., 2002. Nitrogen in aquatic ecosystems. Ambio 31, 102–112.

Rao, A.M., McCarthy, M.J., Gardner, W.S., Jahnke, R.A., 2008. Respiration and denitrification in permeable continental shelf deposits on the south Atlantic bight: N_2: Ar and isotope pairing measurements in sediment column experiments. Cont. Shelf Res. 28, 602–613.

Reisinger, A.J., Tank, J.L., Rosi-Marshall, E.J., Hall Jr., R.O., Baker, M.A., 2015. The varying role of water column nutrient uptake along river continua in contrasting landscapes. Biogeochemistry 125, 115–131.

Reisinger, A.J., Tank, J.L., Hoellein, T.J., Hall, R.O., 2016. Sediment, water column, and open-channel denitrification in rivers measured using membrane-inlet mass spectrometry. J. Geophys. Res. Biogeosci. 121, 1258–1274.

Revsbech, N.P., 1989. An oxygen microsensor with a guard cathode. Limnol. Oceanogr. 34, 474–478.

Roberts, K.L., Kessler, A.J., Grace, M.R., Cook, P.L., 2014. Increased rates of dissimilatory nitrate reduction to ammonium (DNRA) under oxic conditions in a periodically hypoxic estuary. Geochim. Cosmochim. Acta 133, 313–324.

Rotthauwe, J.H., Witzel, K.P., Liesack, W., 1997. The ammonia monooxygenase structural gene amoA as a functional marker: molecular fine-scale analysis of natural ammonia-oxidizing populations. Appl. Environ. Microb. 63, 4704–4712.

Schlesinger, W.H., 2009. On the fate of anthropogenic nitrogen. P. Natl. Acad. Sci. USA 106, 203–208.

Sebilo, M., Billen, G., Mayer, B., Billiou, D., Grably, M., Garnier, J., Mariotti, A., 2006. Assessing nitrification and denitrification in the Seine River and estuary using chemical and isotopic techniques. Ecosystems 9, 564–577.

Seitzinger, S.P., 1988. Denitrification in freshwater and coastal marine ecosystems: ecological and geochemical significance. Limnol. Oceanogr. 33, 702–724.

Seitzinger, S.P., Harrison, J.A., Böhlke, J., Bouwman, A., Lowrance, R., Peterson, B., Tobias, C., Drecht, G.V., 2006. Denitrification across landscapes and waterscapes: a synthesis. Ecol. Appl. 16 (6), 2064–2090.

Sivakumar, B., 2002. A phase-space reconstruction approach to prediction of suspended sediment concentration in rivers. J. Hydrol. 258, 149–162.

Smith, P., 1995. Non-invasive ion probes—tools for measuring transmembrane ion flux. Nature 378, 645.

Turner, R.E., Rabalais, N.N., 1994. Coastal eutrophication near the Mississippi river delta. Nature 368, 619–621.

Vannote, R.L., Minshall, G.W., Cummins, K.W., Sedell, J.R., Cushing, C.E., 1980. The river continuum concept. Can. J. Fish. Aquat. Sci. 37, 130–137.

Venterink, H.O., Hummelink, E., Van den Hoorn, M.W., 2003. Denitrification potential of a river floodplain during flooding with nitrate-rich water: grasslands versus reedbeds. Biogeochemistry 65, 233–244.

Wang, S., Zhu, G., Peng, Y., Jetten, M.S., Yin, C., 2012. Anammox bacterial abundance, activity, and contribution in riparian sediments of the Pearl River estuary. Environ. Sci. Technol. 46, 8834–8842.

Water Conservancy Committee of the Yellow River, 2013. Yellow River Sediment Bulletin. The Yellow River Public House of the Water Resources, Zhengzhou, China.

Xia, X., Dong, J., Wang, M., Xie, H., Xia, N., Li, H., Zhang, X., Mou, X., Wen, J., Bao, Y., 2016. Effect of water-sediment regulation of the Xiaolangdi reservoir on the concentrations, characteristics, and fluxes of suspended sediment and organic carbon in the Yellow River. Sci. Total Environ. 571, 487–497.

Xia, X., Yang, Z., Zhang, X., 2009. Effect of suspended-sediment concentration on nitrification in river water: importance of suspended sediment-water interface. Environ. Sci. Technol. 43, 3681–3687.

Xia, X.H., Liu, T., Yang, Z.F., Zhang, X.Q., Yu, Z.B., 2013. Dissolved organic nitrogen transformation in river water: effects of suspended sediment and organic nitrogen concentration. J. Hydrol. 484, 96–104.

Xia, X.H., Yang, Z.F., Huang, G.H., Zhang, X.Q., Yu, H., Rong, X., 2004. Nitrification in natural waters with high suspended-solid content — a study for the Yellow River. Chemosphere 57, 1017–1029.

Xia, X.H., Zhou, J.S., Yang, Z.F., 2002. Nitrogen contamination in the Yellow River basin of China. J. Environ. Qual. 31, 917–925.

Zhang, Y., Xie, X., Jiao, N., Hsiao, S.Y., Kao, S.J., 2014. Diversity and distribution of amoA-type nitrifying and nirS-type denitrifying microbial communities in the Yangtze River estuary. Biogeosciences 11, 2131–2145.

Zhu, G., Wang, S., Zhou, L., Wang, Y., Zhao, S., Xia, C., Wang, W., Zhou, R., Wang, C., Jetten, M.S., 2015. Ubiquitous anaerobic ammonium oxidation in inland waters of China: an overlooked nitrous oxide mitigation process. Sci. Rep. 5.